Very High-Resolution Imaging of Post-Mortem Human Cardiac Tissue using X-ray Phase Contrast Tomography

I. Mirea[1], F. Varray[1], Y.M. Zhu[1], L. Fanton[1], M. Langer[1,2], P.S. Jouk[3], G. Michalowicz[3], Y. Usson[3] , I. E. Magnin[1]

[1]Université de Lyon, CREATIS; CNRS UMR5220; Inserm U1044; INSA-Lyon; Université Lyon 1, France
[2]European Synchrotron Radiation Facility, Grenoble, France
[3]Université Joseph Fourier, Grenoble, France

Abstract. This paper investigates the 3D microscopic structure of *ex-vivo* human cardiac muscle. Usual 3D imaging techniques such as DMRI or CT do not achieve the required resolution to visualise cardio-myocytes, therefore we employ X-ray phase contrast micro-CT, developed at the European Synchrotron Radiation Facility (ESRF). Nine tissue samples from the left ventricle and septum were prepared and imaged at an isotropic resolution of 3.5 μm, which is sufficient to visualise cardio-myocytes.The obtained volumes are compared with 2D histological examinations, which serve as a basis for interpreting the 3D X-ray phase-contrast results. Our experiments show that 3D X-ray phase-contrast micro-CT is a viable technique for investigating the 3D arrangement of myocytes *ex-vivo* at a microscopic level, allowing a better understanding of the 3D cardiac tissue architecture.

Keywords: phase-contrast imaging, histology, cardio-myocyte

1 Introduction

Cardiovascular diseases remain one of the most serious health problems in the world, motivating research that deepens our understanding of the myocardial function. This requires a good knowledge of the myocardial architecture, especially the myocyte architecture, to understand relations between mechanical function, hemodynamics and adaptive structural changes in cardiac diseases.

Cardiac muscle cells have diameters in the range of 10-20 μm and lengths around 100 μm. To image them, a resolution in the μm range is required. Current imaging techniques can deliver either very high resolution but only in a small field of view, or the entire heart can be imaged to see the overall organisation of the myocytes, but at a resolution that does not show how individual myocytes are arranged.

Optical images of histological sections can deliver high resolution for *ex-vivo* 2D imaging, but they can suffer from distortions due to cutting the thin samples.

Another optical technique, Polarized Light Imaging (PLI), can be used to obtain maps of the orientation of myocardiac cells. In [9, 7], a fetal heart was divided into a set of parallel contiguous slices and each one was imaged with PLI, thus constructing a 3D map of the myocyte orientations in the entire heart at a resolution of 100 μm $\times$ 100 μm $\times$ 500 μm. This resolution remains insufficient for visualizing individual myocytes, and what is actually seen is the averaged orientation of a population of myocytes in each voxel.

Compared with the previous two techniques, Magnetic Resonance Imaging is non-invasive and can be used *in-vivo* to image the entire heart. Diffusion Tensor MRI (DT-MRI) can recover the dominant orientation of myocytes in each voxel because of the stronger diffusion of water molecules in the direction parallel to that of the myocytes. DT-MRI can thus map myocyte orientations throughout the entire heart *in-vivo* and can serve to detect abnormalities [15, 8]. However, the typical spatial resolution is low (1 mm $\times$ 1 mm $\times$ 2 mm) therefore the 3D organization of myocytes at a microscopic level remains unknown. High-resolution MRI setups such as [1] can achieve 30 μm $\times$ 30 μm $\times$ 300 μm or 60 μm $\times$ 60 μm $\times$ 60 μm voxel sizes, however this remains above the diameter of cardio-myocytes.

A new method that has great potential for applications in biomedical imaging is X-Ray Phase Contrast Imaging (PCI). Just as conventional transmission-based X-ray imaging, PCI can be combined with Computed Tomography (CT) techniques to obtain 3D images, and a better contrast is obtained in soft tissue compared to classical CT. Several techniques are now available to exploit and visualize the phase-contrast, of which we mention propagation-based imaging (PBI), also known as in-line holography, which yields high spatial resolution without the need for complex instrumentation. PBI is useful for imaging cardiac tissue because it enhances contrast at myocyte boundaries [4].

Allowing high contrast 3D visualization of thick and complex samples at high spatial resolution, X-Ray PCI can image a wide range of tissues and organs not only *ex-vivo* but also *in-vivo*. In [10], angiographies in the mouse brain were performed at 6 μm resolution. However, most PBI studies use higher resolutions, such as [5] who have visualised *ex-vivo* 3D osteon morphology with a spatial resolution of 1.4 μm. Also interesting are the experiments of [10], who were able to visualize subtle details in the rat brain through a phase retrieval method that allows PBI-CT through a single distance PBI image, with a reduction in absorbed dose and acquisition time. *In-vivo* studies with X-Ray PCI on humans have also been conducted, the first clinical trials for mammography being described in [2]. They show that mammographies with synchrotron radiation can be used to clarify the diagnosis in patients with suspicious breast abnormalities identified by combined digital mammography and ultrasonography.

In our study, we investigate the 3D cardiac tissue structure using X-Ray micro-CT phase contrast imaging based on in-line propagation implemented at the European Synchrotron Radiation Facility (ESRF) [11]. The technique allows to detect the microscopic-scale boundaries of the myocytes in the heart tissue [4].

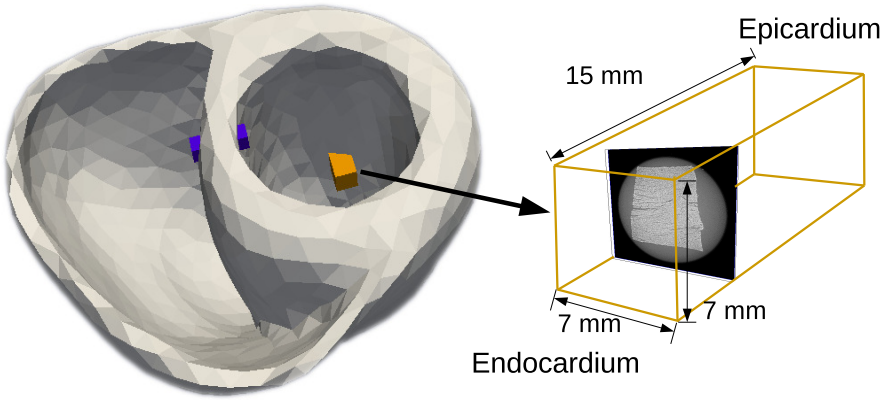

(a) heart sample section

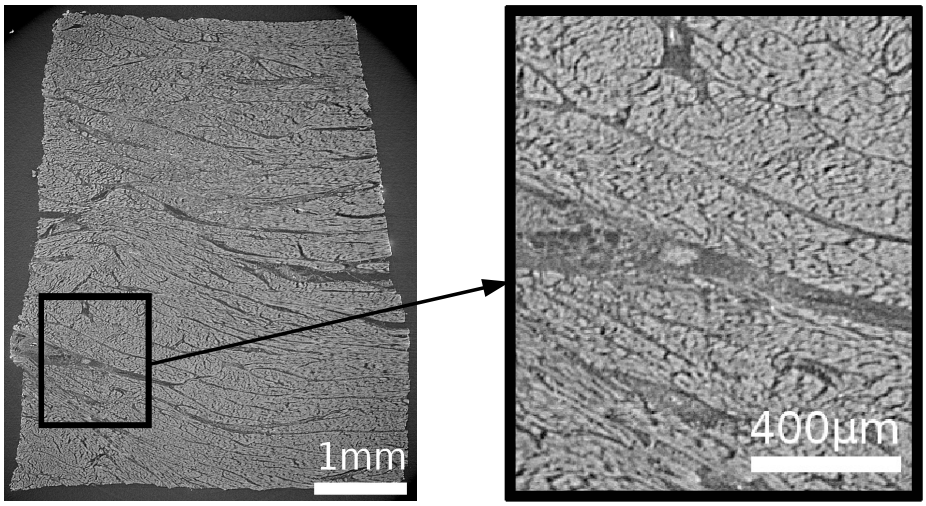

(b) X-ray PCI and a zoomed-in area

Fig. 1: Fig. 1a: schematic representation of the heart sample section at the junction between the apical third and the equatorial third. The sample has a height of 15 mm, corresponding to the thickness of the left ventricle wall, and the sides of about 5-6 mm (7 mm including the outer edges of the image). It is imaged at a resolution of 3.5 μm. Fig. 1b left: X-ray PCI viewed in a plane orthogonal to the epicardium-endocardium direction. The bundle of myocardial cells grossly follows the curvature of the ventricular wall and corresponds mostly to a circular arrangement around the ventricle. Fig. 1b right: at a finer scale, the orientation of myocardial cells can be refined, they are obliquely cut. Myocardial cells appear in white, separated by short and thin dark gaps. The larger, roughly linear dark gaps separate bundles of myocardial cells. The lumen of a blood vessel is also visible as a thick dark gap in the middle of the image.

2 Materials and methods

Human heart samples were supplied by the Medico-Legal Institute of Lyon IML HCL ($n^\circ DC-2012-1588$) and were collected during a medical-legal autopsy of a subject who suffered a violent death. From this heart, 9 samples were collected from the septal, anterior, lateral, and posterior left ventricle, with heights of 11 - 20 mm and 6 mm sides for imaging.

The samples were first immersed in a formalin solution for sterilization. However, previous experience showed that an immersion in alcohol results in better image quality in soft tissue. Therefore, the formaldehyde was rinsed with water, then the samples were immersed in pure water for rehydration. Finally, they were immersed in successive baths of increasing alcoholic concentrations, from 10% to 70%, before being imaged. Image acquisition was performed at ESRF on beamline ID19 using X-ray micro-CT PCI based on in-line propagation [3]. Unfiltered undulator radiation was used, with an average energy of ~ 19 keV and an energy bandwith of $< 10\%$. The detector was placed 1 m from the sample to achieve phase contrast. Image reconstruction was performed using Paganin's method for phase retrieval and filtered backprojection for tomographic reconstruction [13]. Compared with [3] who studied the silicon single crystal and metal matrix composites, we now apply the method to human cardiac tissue and use more recent materials with higher spatial resolution. Our acquisitions are made at a resolution of 3.5 μm $\times$ 3.5 μm $\times$ 3.5 μm.

Due to the maximum height allowed by the detector, 3 or 4 successive acquisitions with an overlap of 97 planes were made by shifting the sample vertically. These were merged to recreate the entire volume. Scan time for each successive acquisition is approximately 25 minutes. For the 15 $mm \times 6$ $mm \times 6$ mm sample in Figure 1 , the total acquisition time is 1 h 17 min. The imaging setup used in this experiment is non-destructive for the sample.

3 Image interpretation

For illustration purposes we choose a sample from the inferior part of the left ventricle, at the junction between the apical third and the equatorial third, as illustrated in Fig. 1a.

Fig. 2a shows a 3D view of a small part of the chosen sample. This part contains $0.44 \cdot 10^9$ voxels for a file size of 1.75 GB. The 3D visualisation was made with CreaTools [6], a software tool created in the CREATIS lab. Three orthogonal planes are shown in order to illustrate different types of details that can be seen. The plane orthogonal to the X axis illustrates projections of myocyte orientations appearing as long, thin filaments. The lumen of a blood vessel can be seen with round shaped erythrocytes.

Fig. 3a illustrates a zoomed-in area of another plane orthogonal to the X axis. Again, we see the lumen of a blood vessel (arrow *1*), a capillary with red blood cells (arrow *2*), projections of myocyte orientations in high detail, as thin white filaments (arrows *3*), and intercellular space, as black filaments (arrows *4*).

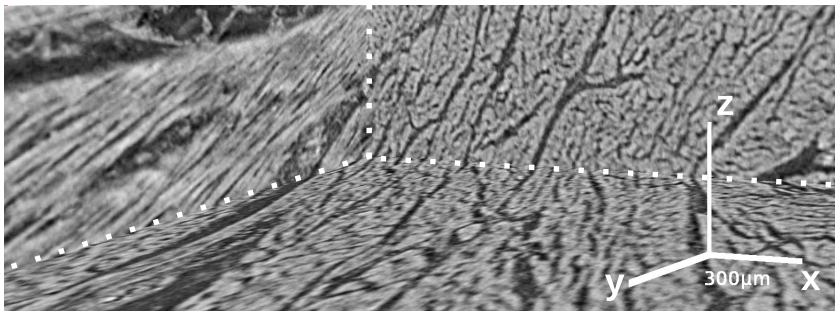

(a) original 3D image

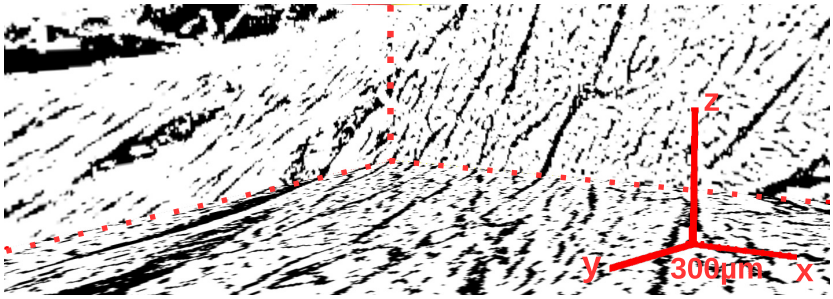

(b) after Otsu segmentation

Fig. 2: 2a: X-ray phase contrast 3D image of a heart sample from the inferior part of the lateral wall of the left ventricle. 2b: segmentation of myocardial cells using the Otsu thresholding method with two thresholds [12].

Fig. 3c is also from the same volume as Fig. 2a, but in a plane orthogonal to the Y axis. In this figure myocytes are separated by short, thin, curved dark areas, and bundles of myocytes separated by thicker, long and straight dark zones. A blood vessel is also visible as a thick dark band in the left part of the image.

The obtained phase contrast images are suitable for automatic analysis. For illustration purposes, the Otsu thresholding method [12] was applied to segment myocytes in Fig. 2b. This result is already good considering the 3D aspect of the problem, the large number of voxels and the simplicity of the method. More complex segmentation methods could highlight the separation between myocytes even better. Thresholding is easier in 2D, as shown in Fig. 4. Other types of information can also be extracted from phase contrast images, such as the 3D orientation of myocytes throughout the volume [14].

It is interesting to compare the X-ray phase contrast images with optical images of histological sections. To this end, Fig. 3b depicts such a histological image taken from approximately the same area of the heart as Fig. 3a and with a similar slice orientation. Fig. 3d is another histological section, but with approximately the same localisation and orientation as Fig. 3c. The two image

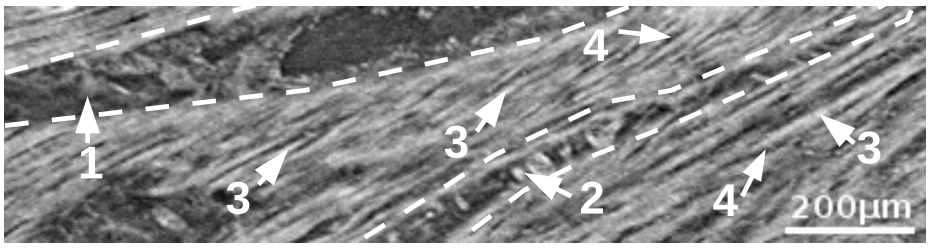

(a) X-ray phase contrast image, X plane

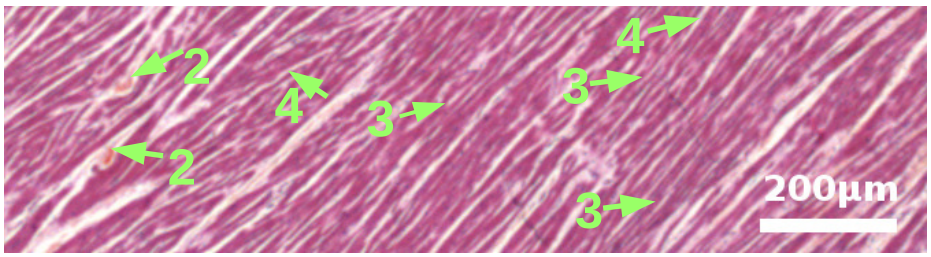

(b) histological section, X plane

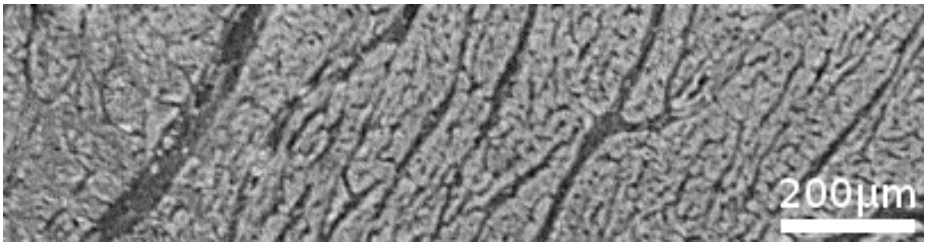

(c) X-ray phase contrast image, Y plane

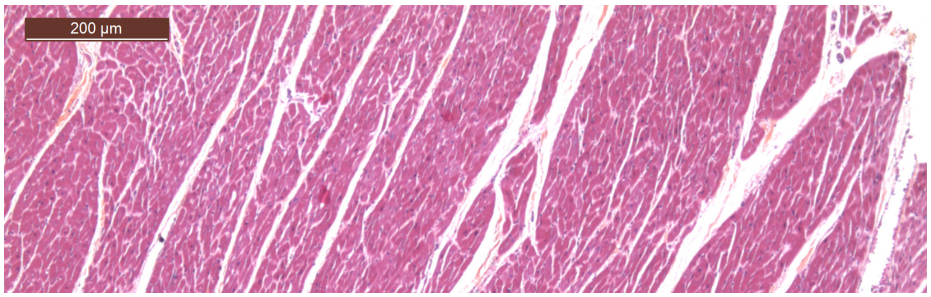

(d) histological section, Y plane

Fig. 3: Fig. 3a: X-ray phase contrast image section perpendicular to the X axis (see Fig. 2a); *1* - blood vessel; *2* - capillary with red blood cells; *3* - projections of myocyte orientations (white); *4* - intercellular space (black). Fig. 3b: histological section similar to Fig. 3a. Both Fig. 3a and Fig. 3b show myocytes as thin long filament-like structures. Fig. 3c: X-ray phase contrast image section perpendicular to the Y axis. Fig. 3d: histological section similar to Fig. 3c. Both Fig. 3c and Fig. 3d show myocytes and bundles of myocytes.

Fig. 4: Binary thresholding of Fig. 3c with a manually-chosen threshold.

pairs in Fig. 3 are structurally similar. In the above pair, myocytes appear as long, filament-like structures (white in the X-ray phase-contrast images, red in the optical images). The separation between myocytes appears as thin, black lines in Fig. 3a and as thin, white lines in Fig. 3b. For the other image pair, myocytes are separated by thin, short, curved areas, and bundles of myocytes are separated by long, straight areas.

4 Conclusion

We have shown that X-ray phase contrast images are a viable tool for examining the microstructure of the heart. They can show the same structures as those seen in histological sections, without having to carefully prepare a set of slices. The greatest advantage of X-ray phase contrast images is the ability to capture 3D structures, from which much more information can be extracted, either through visual inspection by a human expert or through analysis with automatic algorithms.

Acknowledgements

We would like to thank F. Peyrin, C. Olivier and M. Ozon for technical support at ESRF Grenoble. This study was funded by the French National Research Agency (ANR) through the MOSIFAH project (Multimodal and multiscale modeling and simulation of the fibre architecture of the human heart, ANR-13-MONU-0009).

References

1. Baltes, C., Radzwill, N., Bosshard, S., Marek, D., Rudin, M.: Micro mri of the mouse brain using a novel 400mhz cryogenic quadrature rf probe. NMR in Biomedicine 22(8), 834–842 (2009), http://dx.doi.org/10.1002/nbm.1396
2. Castelli, E., Tonutti, M., Arfelli, F., Longo, R., Quaia, E., Rigon, L., Sanabor, D., Zanconati, F., Dreossi, D., Abrami, A., Quai, E., Bregant, P., Casarin, K., Chenda, V., Menk, R.H., Rokvic, T., Vascotto, A., Tromba, G., Cova, M.A.: Mammography with synchrotron radiation: First clinical experience with phase-detection technique. Radiology 259(3), pp. 684–694 (2011)

3. Cloetens, P., Pateyron, M., Buffière, J.Y., Peix, G., Baruchel, J., Peyrin, F., Schlenker, M.: Observation of microstructure and damage in materials by phase sensitive radiography and tomography. Journal of Applied Physics 81(9), pp. 5878–5886 (1997)
4. Cloetens, P., Ludwig, W., Baruchel, J., Guigay, J.P., Pernot-Rejmnkov, P., Salom-Pateyron, M., Schlenker, M., Buffire, J.Y., Maire, E., Peix, G.: Hard x-ray phase imaging using simple propagation of a coherent synchrotron radiation beam. Journal of Physics D: Applied Physics 32(10A), A145 (1999)
5. Cooper, D.M.L., Erickson, B., Peele, A., Hannah, K., Thomas, C.D.L., Clement, J.G.: Visualization of 3D osteon morphology by synchrotron radiation micro-CT. Journal of Anatomy 219(4), pp. 481489 (2011)
6. Dávila Serrano, E., Guigues, L., Roux, J.P., Cervenansky, F., Camarasu-Pop, S., Riveros Reyes, J., Flrez-Valencia, L., Hernndez Hoyos, M., Orkisz, M.: Creatools: A framework to develop medical image processing software: Application to simulate pipeline stent deployment in intracranial vessels with aneurysms 7594, 55–62 (2012)
7. Desrosiers, P.A., Michalowicz, G., Jouk, P.S., Usson, Y., Zhu, Y.: Modeling of the optical behavior of myocardial fibers in polarized light imaging. In: Statistical Atlases and Computational Models of the Heart. Imaging and Modelling Challenges, Lecture Notes in Computer Science, vol. 7746, pp. pp. 235–244 (2012)
8. Ferreira, P., Kilner, P., McGill, L.A., Nielles-Vallespin, S., Scott, A., Ho, S., McCarthy, K., Haba, M., Ismail, T., Gatehouse, P., de, S.R., Lyon, A., Prasad, S., Firmin, D., Pennell, D.: In vivo cardiovascular magnetic resonance diffusion tensor imaging shows evidence of abnormal myocardial laminar orientations and mobility in hypertrophic cardiomyopathy. Journal of Cardiovascular Magnetic Resonance 16(1), pp. 87 (2014)
9. Jouk, P.S., Mourad, A., Milisic, V., Michalowicz, G., Raoult, A., Caillerie, D., Usson, Y.: Analysis of the fiber architecture of the heart by quantitative polarized light microscopy: Accuracy, limitations and contribution to the study of the fibre architecture of the ventricles during fetal and neonatal life. Eur. J. Cardio-Thorac. Surg. 31(5), pp. 915–921 (2007)
10. Kidoguchi, K., Tamaki, M., Mizobe, T., Koyama, J., Kondoh, T., Kohmura, E., Sakurai, T., Yokono, K., Umetani, K.: In vivo x-ray angiography in the mouse brain using synchrotron radiation. Stroke 347, pp. 1856–1861 (2006)
11. Langer, M., Cloetens, P., Pacureanu, A., Peyrin, F.: X-ray in-line phase tomography of multimaterial objects. Optics Letters 37(11), pp. 2151–2153 (2012)
12. Otsu, N.: A threshold selection method from gray-level histograms. IEEE Transactions on Systems, Man, and Cybernetics 9(1), pp. 62–66 (1979)
13. Paganin, D., Mayo, S.C., Gureyev, T.E., Miller, P.R., Wilkins, S.W.: Simultaneous phase and amplitude extraction from a single defocused image of a homogeneous object. Journal of Microscopy 206(1), 33–40 (2002)
14. Varray, F., Wang, L., Fanton, L., Zhu, Y.M., Magnin, I.E.: High resolution extraction of local human cardiac fibre orientations. In: Proceedings of the 7th International Conference on Functional Imaging and Modeling of the Heart. pp. 150–157 (2013)
15. Wang, L., Zhu, Y., Li, H., Liu, Y., Magnin, I.E.: Multiscale modeling and simulation of the cardiac fiber architecture for dmri. IEEE Transactions on Biomedical Engineering 59(1), pp. 16–19 (2012)